



Imaging-based cavity optomechanics

Item Type	Proceedings; text
Authors	Pluchar, C.M.; Agrawal, A.R.; Wilson, D.J.
Citation	Christian M. Pluchar, Aman R. Agrawal, Dalziel J. Wilson, "Imaging-based cavity optomechanics," Proc. SPIE 12649, Optical Trapping and Optical Micromanipulation XX, 1264907 (5 October 2023); doi: 10.1117/12.2676081
DOI	10.1117/12.2676081
Publisher	SPIE
Journal	Proceedings of SPIE - The International Society for Optical Engineering
Rights	© 2023 SPIE.
Download date	30/08/2024 04:54:10
Item License	http://rightsstatements.org/vocab/InC/1.0/
Version	Final Published Version
Link to Item	http://hdl.handle.net/10150/671354

PROCEEDINGS OF SPIE

SPIDigitalLibrary.org/conference-proceedings-of-spie

Imaging-based cavity optomechanics

Christian Pluchar, Aman Agrawal, Dalziel Wilson

Christian M. Pluchar, Aman R. Agrawal, Dalziel J. Wilson, "Imaging-based cavity optomechanics," Proc. SPIE 12649, Optical Trapping and Optical Micromanipulation XX, 1264907 (5 October 2023); doi: 10.1117/12.2676081

SPIE.

Event: SPIE Nanoscience + Engineering, 2023, San Diego, California, United States

Imaging-based cavity optomechanics

Christian M. Pluchar, Aman R. Agrawal, and Dalziel J. Wilson

Wyant College of Optical Sciences, University of Arizona, Tucson, AZ 85716

ABSTRACT

Cavity optomechanics has led to advances in quantum sensing, optical manipulation of mechanical systems, and macroscopic quantum physics. However, previous studies have typically focused on cavity optomechanical coupling to translational degrees of freedom, such as the drum mode of a membrane, which modifies the amplitude and phase of the light field. Here, we discuss recent advances in “imaging-based” cavity optomechanics – where information about the mechanical resonator’s motion is imprinted onto the spatial mode of the optical field. Torsion modes are naturally measured with this coupling and are interesting for applications such as precision torque sensing, tests of gravity, and measurements of angular displacement at and beyond the standard quantum limit. In our experiment, the high- Q torsion mode of a Si_3N_4 nanoribbon modulates the spatial mode of an optical cavity with degenerate transverse modes. We demonstrate an enhancement of angular sensitivity read out with a split photodetector, and differentiate the “spatial” optomechanical coupling found in our system from traditional dispersive coupling. We discuss the potential for imaging-based quantum optomechanics experiments, including pondermotive squeezing and quantum back-action evasion in an angular displacement measurement.

Keywords: cavity optomechanics, quantum optomechanics, optical lever, quantum imaging, nanomechanics

1. INTRODUCTION

Mechanical resonators coupled to optical cavities enable strong interactions between mechanical and optical modes, studied extensively within cavity optomechanics.¹ Notable demonstrations include manipulation of mechanical degrees of freedom through optical spring and damping effects,² ground state preparation of mechanical modes via coherent cavity cooling,³ and measurements at and below the standard quantum limit.⁴ Key advances

Send correspondence to: cpluchar@arizona.edu, dalziel.wilson@gmail.com

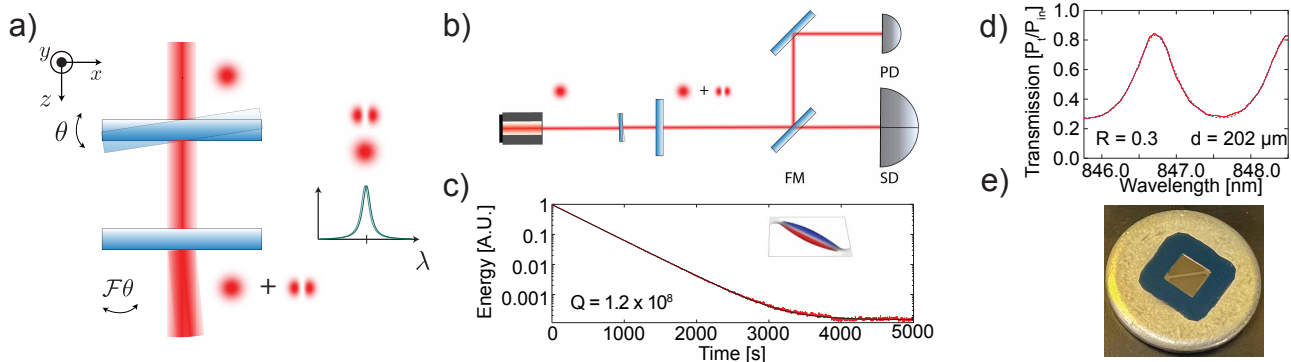


Figure 1. Experiment overview. a) Spatial mode cavity optomechanical coupling: with an injected HG_{00} mode, the angular motion of a Fabry-Perot cavity mirror produces an HG_{10} component to the field, both of which resonate simultaneously inside the plano-plano cavity. The cavity amplifies the HG_{10} mode, increasing sensitivity to the angular motion of the mirror. b) Readout schematic, which includes both a photodetector (PD) and split photodetector (SD) for analyzing the transmitted field, switched between uSi_3N_4 a flipper mirror (FM). c) Ringdown measurement of the torsion mode (inset) of our device, with a fit to the data (black) indicating $Q = 1.2 \times 10^8$. d) Cavity transmission fringe ($F = 3.2$) cavity, with a model (dashed blue) used to infer the cavity parameters of $\mathcal{F} = 3.2$ and length $202\mu\text{m}$. e) Picture of the device, with a $400\mu\text{m}$ wide nanoribbon on top of a membrane, forming a plano-plano cavity.

facilitated by cavity optomechanics include gravitational wave detectors⁵ and emerging quantum technologies such as optical-to-microwave transducers.⁶

Cavity optomechanics typically focuses on the dispersive interaction between the mechanical and optical modes, characterized by the coupling of mechanical modes to the phase of a single cavity mode. However, some mechanical modes, including metrologically significant torsion modes,⁷ may only experience weak dispersive coupling due to their net-zero center of mass motion. Inspired by the discovery of high- Q torsion modes in silicon nitride (Si_3N_4) nanoribbons,⁸ we explore coupling nanomechanical torsion modes to an optical cavity. In our experiment, the mechanical motion converts some of the intracavity fundamental Hermite-Gauss (HG) mode into the HG_{10} mode, which we then image to readout the torsion motion.⁹ This is a demonstration of “spatial” optomechanical coupling to an optical cavity in which two orthogonal spatial modes are coherently coupled via the mechanical motion.¹⁰ To maximize the sensitivity, the short, plano-plano geometry of our cavity enables nearly frequency-degenerate transverse optical modes. We can distinguish between spatial and dispersive optomechanical coupling in our system by selecting our readout scheme (photodetector versus split photodetector) and the detuning dependence.

Borrowing tools from the field of quantum imaging, our work represents a step towards “imaging-based” optomechanics, in which the mechanical mode interacts with the spatial mode of the light field. In contrast to previous studies within both quantum imaging and quantum optomechanics, the “scene” we image is altered by the spatial fluctuations of the radiation pressure of the incident field. By utilizing nanomechanical oscillators, our experimental platform positions us to access effects produced by radiation pressure including quantum backaction and pondermotive squeezing.¹¹ Our experiment also demonstrates an approach to realize angular displacement measurements at the standard quantum limit and exploring novel detection schemes utilizing the spatial degree of freedom of light, which has recently been shown to be important in some levitated optomechanics experiments.^{12–14}

2. OPTOMECHANICAL COUPLING OF A TORSION OSCILLATOR TO AN OPTICAL CAVITY

In this section, we study optomechanical coupling of a torsion oscillator to an optical cavity, revealing it to be a form of coherent coupling between two different spatial modes of an optical cavity. Our torsion oscillator is the torsion mode of a ribbon, enabled by the Si_3N_4 nanoribbons used in our experiment. The modeshape of the fundamental torsion mode is given by⁸

$$\theta(y) = \sin(\pi y/L) \quad (1)$$

where θ is the angle of rotation around the y -axis and L is the length of the ribbon. We perform our measurements in the center of the ribbon, where $\theta(y)$ is maximized.

An optical field reflected off the ribbon of amplitude reflectivity r_f experiences a phase shift $e^{ik\theta x}$. For an incident field in the fundamental Hermite-Gauss (HG) mode, the reflected field is

$$E(x, y, z) = A_{00} r_f \frac{\sqrt{2/\pi}}{w(z)} e^{-\frac{(x^2+y^2)}{w^2(z)}} e^{ik\theta x} \approx (1 + ik\theta x) A_{00} r_f \frac{\sqrt{2/\pi}}{w(z)} e^{-\frac{(x^2+y^2)}{w^2(z)}}, \quad (2)$$

where A_{00} is the incident electric field amplitude, with power equal to $|A_{00}|^2 = P$, $w(z)$ is the spot size and $k = 2\pi/\lambda$ is the wavenumber, and we have assumed that the displacement relative to the wavelength λ is small. Notably, a field centered on the nanoribbon experiences a net zero phase shift, implying a negligible dispersive optomechanical coupling $G = \partial\omega_c/\partial z \approx 0$, where ω_c is the cavity resonance frequency. Instead, we can estimate θ by examining the spatial mode of the optical field. Writing the reflected field as an expansion of HG modes shows that the reflection produces a superposition of two orthogonal modes

$$\begin{aligned} E(x, y, z) &= A_{00} r_f \frac{\sqrt{2/\pi}}{w(z)} e^{-\frac{(x^2+y^2)}{w^2(z)}} + A_{10}^\theta \frac{2x}{w(z)} \frac{\sqrt{2/\pi}}{\pi w(z)} e^{-\frac{(x^2+y^2)}{w^2(z)}}, \\ &= A_{00} r_f E_{00}(x, y, z) + A_{10}^\theta E_{10}(x, y, z), \end{aligned} \quad (3)$$

where

$$A_{10}^\theta = ikw_0\theta A_{00}r_f, \quad (4)$$

is the amplitude of the HG₁₀ mode and $E_{00,10}(x, y, z)$ describe the modeshapes of the HG_{00,10} modes. A_{10}^θ can be measured with a split detector or another spatially-resolving measurement scheme such as a homodyne interferometer with the local oscillator in the HG₁₀ mode.¹⁵

Next, we examine a Fabry-Perot resonator with a mirror that is free to rotate (Fig. 1a). The input field is in the HG₀₀ mode, but by rotating the compliant mirror, a small amount of HG₁₀ is generated in the intracavity field. The HG₁₀ mode amplitude of the transmitted field of the cavity is given by⁹

$$A_{t1} = iA_{00}\theta kw_0 \frac{r_e r_f t_f t_e e^{\frac{1}{2}i(\xi+2\phi)}}{(-1 + r_e r_f e^{i\phi}) (-1 + r_e r_f e^{i(\xi+\phi)}), \quad (5)$$

where A_{00} is the amplitude of the fundamental mode, r_f, r_e, t_f , and t_e are the front and end mirror reflection and transmission coefficients respectively, ϕ is the detuning from resonance, and $\xi = \arctan[z/z_R]$ is the relative Gouy phase between the HG₀₀ and HG₁₀ modes inside the cavity, with z_R being the Rayleigh length. A non-zero value of ξ will decrease the magnitude of the transmitted HG₁₀ component of the field. For an impedance matched and lossless cavity ($r_e = r_f$ and $t_e = t_f$) where both optical modes are degenerate, Eq. 5 simplifies to

$$A_{t1} = iA_{00}\theta kw_0 \frac{r_f^2 t_f^2 e^{i\phi}}{(-1 + r_f^2 e^{i\phi})^2} \quad (6)$$

so that the magnitude of the HG₁₀ mode is proportional to the the motion θ , the input mode amplitude A_{i0} and the waist. Eq. 6 is maximized on resonance, and for a lossless cavity reduces to:

$$A_{t1}^{\phi=0} = iA_{00}\theta kw_0 \frac{r_f^2}{(1 - r_f^2)}. \quad (7)$$

Comparing to Eq. 4, this gives an enhancement of the HG₁₀ mode amplitude of

$$\frac{A_{t1}^{\phi=0}}{A_{10}} = \frac{r_f}{1 - r_f^2} = \frac{\mathcal{F}}{r_f \pi}, \quad (8)$$

where \mathcal{F} is the cavity finesse. This will improve measurements of the angular displacement for large values of \mathcal{F} .

3. EXPERIMENT

We now explore readout nanomechanical motion using spatial mode coupling to an optical cavity. Our device is a ‘‘ribbon-on-a-membrane’’ (ROM) optomechanical system formed by a 400 μm wide Si₃N₄ ribbon and 5 mm square membrane on opposite sides of a Si chip, forming a plano-plano Fabry-Perot cavity. The chip is 200 μm thick and both Si₃N₄ films are 75 nm thick, resulting in an estimated power reflectivity of $|r_f|^2 = .33$. A picture of the device is shown in Fig. 1e. We focus on the fundamental torsion mode of the ribbon and find a mechanical resonance frequency $\omega_m = 2\pi \times 52.42$ kHz and $Q = 1.2 \times 10^8$ at high vacuum using a ringdown measurement (shown in Fig. 1c). The ROM cavity is nearly impedance matched due to the low loss of the cavity and identical reflectivity of the two surfaces, and we observe an interference fringe in transmission, shown in Fig. 1d. The cavity has length 202 μm and finesse $\mathcal{F} = 3.2$ based on a model fit to the fringe (dashed blue), in good agreement with the expected length and finesse. We note that we collect roughly 2.5 times more incident light in transmission compared to reflecting light off the ribbon without a cavity.

To study spatial versus dispersive optomechanical coupling, we make measurements with two different photodetectors while varying the laser-cavity detuning: first, we tune our laser into resonance with the cavity, align our optical beam to the center of the ribbon, and examine the torsion mode motion, shown in Fig. 2a. We calibrate our measurement to the thermal variance $\sigma_\theta^2 = k_B T / I \omega_m^2$, assuming a temperature of 300 K and moment of inertia $I = 3.8 \times 10^{-18}$ kg m² (see SI of⁸). We observe an ~ 80 dB improvement in the SNR using the split detector over the direct detector. We attribute this to the low dispersive coupling of the torsion mode to the

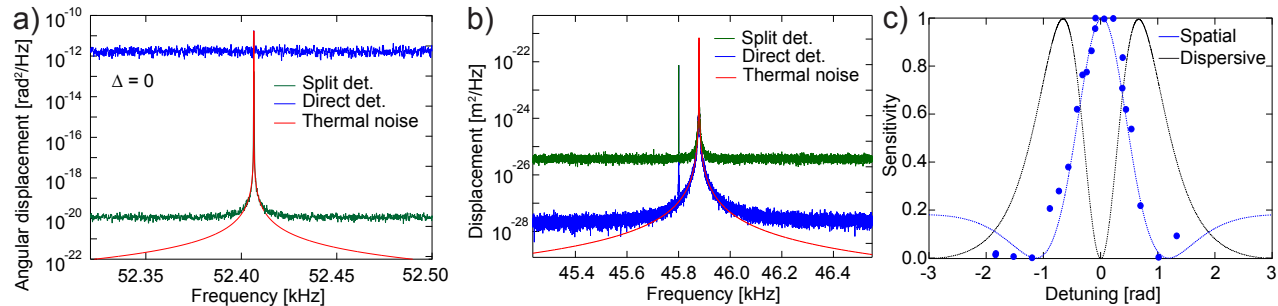


Figure 2. a) Readout of the torsion mode with both a split detector and direct detection, showing large coherent coupling but low dispersive coupling. b) Readout of the flexural mode with direct detection, showing large dispersive coupling. c) Normalized sensitivity versus detuning measuring the torsion mode with the split detector, showing good agreement with the model for the coherent cavity coupling. We also overlay a model for dispersive cavity coupling with direct detection in black for comparison.

cavity, and because the intensity fluctuations caused by dispersive coupling are low on resonance. We note that for an optical lever measurement in transmission without a cavity, the torsion motion would not be observable.

Next, we vary the laser-cavity detuning and monitor the output field with a split detector, as shown in Fig. 2c. We compare our sensitivity to a model assuming spatial optomechanical coupling (approximately given by Eq. 6), which shows good agreement near resonance. We contrast our measurements to dispersive optomechanical coupling to the optical cavity and direct detection (black), which does not resolve variations in the transmitted field. The two are clearly distinguishable, suggesting that the torsion mode experiences spatial mode optomechanical coupling to the cavity.

Finally, we explore traditional dispersive optomechanical coupling in our system. The ribbon has many mechanical modes, including flexural modes (of interest in most optomechanics experiments¹). Instead of altering the spatial mode of the cavity field, the flexural mode modulates the phase, producing intensity fluctuations in the transmitted field. In Fig. 2b, we demonstrate sensitivity to the thermal motion of the flexural mode by measuring the intensity fluctuations using a direct photodetector. Switching to the split photodetector, which suppresses classical intensity noise, our SNR decreases by ~ 20 dB, suggesting the flexural mode is dispersively coupled to the cavity, as expected.

4. CONCLUSION

We demonstrate spatial optomechanical coupling of a nanomechanical resonator to an optical cavity using a torsion oscillator coupled to a Fabry-Perot cavity. The increased interaction strength of torsion modes to optical cavities enables possibilities such as improved measurement sensitivities and studying angular displacement sensing at the standard quantum limit. Our experiment also fits into the larger and emerging framework of imaging-based optomechanics, in which mechanical modes modulate the spatial modes of light.

ACKNOWLEDGMENTS

This work is supported by NSF grant 2239735. CMP wishes to thank the ARCS Foundation for its support. The authors also wish to thank Wenhua He for helpful discussions. Finally, the reactive ion etcher used for this study was funded by an NSF MRI grant, ECCS-1725571.

REFERENCES

- [1] Aspelmeyer, M., Kippenberg, T. J., and Marquardt, F., "Cavity optomechanics," *Rev. Mod. Phys.* **86**(4), 1391–1452.
- [2] Corbitt, T., Chen, Y., Innerhofer, E., Müller-Ebhardt, H., Ottaway, D., Rehbein, H., Sigg, D., Whitcomb, S., Wipf, C., and Mavalvala, N., "An All-Optical Trap for a Gram-Scale Mirror," *Phys. Rev. Lett.* **98**(15), 150802.

- [3] Chan, J., Alegre, T. P. M., Safavi-Naeini, A. H., Hill, J. T., Krause, A., Gröblacher, S., Aspelmeyer, M., and Painter, O., “Laser cooling of a nanomechanical oscillator into its quantum ground state,” *478*(7367), 89–92.
- [4] Mason, D., Chen, J., Rossi, M., Tsaturyan, Y., and Schliesser, A., “Continuous force and displacement measurement below the standard quantum limit,” *Nat. Phys.* **15**(8), 745–749.
- [5] Collaboration, L. S. and Collaboration, V., “Observation of Gravitational Waves from a Binary Black Hole Merger,” *Phys. Rev. Lett.* **116**(6), 061102.
- [6] Barzanjeh, S., Xuereb, A., Gröblacher, S., Paternostro, M., Regal, C. A., and Weig, E. M., “Optomechanics for quantum technologies,” *Nat. Phys.* **18**(1), 15–24.
- [7] Adelberger, E., Gundlach, J., Heckel, B., Hoedl, S., and Schlamminger, S., “Torsion balance experiments: A low-energy frontier of particle physics,” *Progress in Particle and Nuclear Physics* **62**(1), 102–134.
- [8] Pratt, J. R., Agrawal, A. R., Condos, C. A., Pluchar, C. M., Schlamminger, S., and Wilson, D. J., “Nanoscale Torsional Dissipation Dilution for Quantum Experiments and Precision Measurement,” **13**(1).
- [9] Shimoda, T., Miyazaki, Y., Enomoto, Y., Nagano, K., and Ando, M., “Coherent angular signal amplification using an optical cavity,” *Appl. Opt.* **61**(13), 3901.
- [10] Li, X., Korobko, M., Ma, Y., Schnabel, R., and Chen, Y., “Coherent coupling completing an unambiguous optomechanical classification framework,” *Phys. Rev. A* **100**(5), 053855.
- [11] Hao, S. and Purdy, T., “Back-action evasion in optical lever detection,” *ArXiv preprint* (2212.08197).
- [12] Militaru, A., Rossi, M., Tebbenjohanns, F., Romero-Isart, O., Frimmer, M., and Novotny, L., “Ponderomotive Squeezing of Light by a Levitated Nanoparticle in Free Space,” *Phys. Rev. Lett.* **129**(5), 053602.
- [13] Magrini, L., Camarena-Chávez, V. A., Bach, C., Johnson, A., and Aspelmeyer, M., “Squeezed Light from a Levitated Nanoparticle at Room Temperature,” *Phys. Rev. Lett.* **129**(5), 053601.
- [14] Minowa, Y., Kato, K., Ueno, S., Penny, T. W., Pontin, A., Ashida, M., and Barker, P. F., “Imaging based feedback cooling of a levitated nanoparticle,” *Rev. Sci. Instrum.* **93**.
- [15] Delaubert, V., Treps, N., Lassen, M., Harb, C. C., Fabre, C., Lam, P. K., and Bachor, H. A., “TEM₁₀ homodyne detection as an optimal small displacement and tilt measurements scheme,” *Phys. Rev. A* **74**(5), 053823.